CALCULATED EVALUATION OF STRESS-STRAIN STATES OF WELDED JOINTS OF ALUMINIUM AMg61 ALLOY UNDER THE ACTION OF ELECTRODYNAMIC TREATMENT OF WELD METAL IN THE PROCESS OF FUSION WELDING

L.M. Lobanov[1], M.O. Pashchyn[1], O.L. Mikhodui[1], A.A. Hryniuk[1], E.V. Illyashenko[1], P.V. Goncharov[1], V.V. Savytskyi[1], Yu.M. Sydorenko[2], P.R. Ustymenko[2]

[1]National Technical University of Ukraine "Igor Sikorsky Kyiv Polytechnic Institute"
37 Peremohy Prosp., 03056, Kyiv, Ukraine
[2]E.O. Paton Electric Welding Institute of the NASU
11 Kazymyr Malevych Str., 03150, Kyiv, Ukraine

ABSTRACT

The calculated evaluation of effect of impact interaction of the electrode-indenter with a welded plate of AMg61 alloy at its electrodynamic treatment (EDT) in the conditions of elevated temperatures was carried out. The solution of the problem was carried out in a flat two-dimensional Lagrangian statement based on a previously developed mathematical model using ANSYS/LS-DYNA software. The thermal cycle of welding was set by mechanical characteristics of AMg61 alloy at temperatures of 150 and 300 °C. The results of the calculation of residual stresses during impact action of the electrode-indenter at room and elevated temperatures in preliminary tensioned plates of AMg61 alloy of 3 mm thickness were presented. It is shown that the most acceptable temperature (from the studied temperature values) for the electrodynamic treatment of AMg61 alloy is 150 °C. Based on the results of the studies, it was found that the electrodynamic treatment of a welded joint specimen in the form of a plate preliminary loaded with elastic tension, leads to the transition of residual welding tensile stresses into compression stresses.

KEYWORDS: electrodynamic treatment, residual welding stresses, aluminium alloy, electric current pulse, impact interaction, finite-element model, electrode-indenter, elastic-plastic flow theory, fusion welding.

INTRODUCTION

The relevance of the problem of regulating residual welding stresses and strains in structures of aluminium alloys is caused by an increase in their use in various fields of mechanical engineering. Traditional technologies for reducing the level of residual welding stresses based on the mechanical or thermal effect on the welded joint metal is associated with significant difficulties [1, 2].

A challenging method of regulating stress-strain states of welded structures is electrodynamic treatment (EDT) of welded joints, whose efficiency in increasing the accuracy and service life of light alloys is proven in [3, 4]. In EDT, the weld metal is subjected to a volumetric electrodynamic effect, which initiates an electroplastic effect (EPE) in the treatment zone and, as a consequence, the relaxation of residual welding stresses [5].

The use of EDT, taking into account the features of the process of welding, is a new trend of engineering practice, which facilitates an expansion of the capabilities of the method. The study of measures aimed at improving the efficiency of the EDT process is relevant, one of which is the accompanying heating of the electric-pulse effect zone, which, according to data [6], stimulates the mechanisms for relaxation of tensile stresses of low-carbon steel specimens.

The realization of EDT technology in the process of welding contributes to more intensive relaxation of welding stresses as a result of EDT as compared to the treatment of the weld metal at room temperature. It should be noted that until now, the theoretical and experimental studies of the effect of heat from the source of welding heating on the efficiency of EDT use as a method of regulating residual welding stresses have not been carried out. The search for the optimal EDT mode in the conditions of welding is associated with the experimental evaluation of electrophysical and mechanical characteristics of the material being treated. An alternative solution to the problem is the mathematical modeling of the EDT process, which allows evaluating the evolution of stress-strain states of welded joints as a result of EDT [7–9]. This is relevant for optimizing the technology of metal structure treatment in the conditions of their welding.

The aim of the work is the calculated evaluation of stress-strain states of metal materials under the effect of EDT in the process of welding (at elevated temperatures).
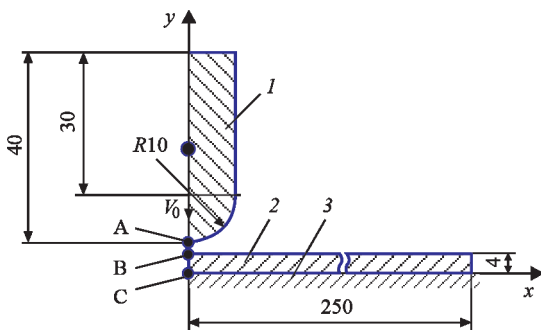
Figure 1. Calculation scheme of the process of dynamic loading of the plate during EDT: *1* — electrode-indenter; *2* — treated specimen; *3* — absolutely rigid base; A — point on the outer surface of the indenter-electrode; B — point on the outer surface of the plate; C — point on the back surface of the plate; V_0 — speed of movement of the indenter-electrode [11]

MATHEMATICAL MODEL AND DISCUSSION OF CALCULATION RESULTS

Modeling of stress-strain states of welded joints as a result of EDT in the conditions of elevated temperatures is performed using a simplified two-dimensional (2D) flat statement. The calculation scheme of the problem of the process of impact interaction of the electrode-indenter with the plates [7] is presented in Figure 1. The solution of the problem was performed with the use of ANSYS/LS-DYNA software. To construct a finite-element mesh, a flat two-dimensional finite element SOLID 162 in the form of a rectangle was used. Computer modeling was performed on the base of a Lagrangian approach using a moving finite-element mesh, which is rigidly related to the environment and deforms together with it [10, 11].

The presence of a geometric symmetry of the electrode *1* and the plate *2*, being in impact interaction, allows considering only half of their cross-section in the calculation scheme with a simultaneous imposition of boundary conditions.

These conditions include the imposition of a prohibition on the movement of nodes of a finite-element mesh (FEM) of the bodies located on the symmetry axis, in the horizontal direction *X*. Leaning of a welded joint against an absolutely rigid base *3* (Figure 1) was considered, which in the mathematical statement is equivalent to the prohibition of FEM-nodes on the movement in the vertical direction *Z*, which belong to

the lower surface of the plate *2*, which contacts with the desktop *3*.

For numerical modeling, a continuous model of elastic-plastic environment (of a plate) under study was used. This allowed recording the laws of mass conservation, amount of movement and energy in the form of differential equations in partial derivatives. To study the processes associated with large plastic deformations of the environment, the theory of plastic flow was used, considering plastic deformation of a solid body as a state of movement on the base of respective Prandtl–Reuss ratios [7].

As an experimental metal material of a welded plate, AMg61 alloy of Al–Mg system was used.

In the mathematical statement, the behavior of the plate materials (aluminium AMg61 alloy) and the electrode-indenter (M1 copper) under the action of external pulse load was described using the ideal elastic-plastic model of the material [9–11]. This model in the library of ANSYS/LS-DYNA software materials is called PLASTIC-KINEMATIC.

The thermal effect was applied on the plate by variation of the values of elasticity modulus *E* and yield strength σ_y of AMg61 alloy at the values of temperature $T = 150$ and 300 °C. The mechanical characteristics of the metal materials involved in modeling at different values of temperature *T* are given in Table 1.

The choice of *T* values is predetermined by modeling the use of EDT in combination with the process of welding, where the specified *T* values correspond to the location of the electrode-indenter along the weld line at a distance L_{EDT} behind the source of welding heating (Figure 2). Modeling of the stress state was also performed for the values of *E* and σ_y at $T = 20$ °C with the aim of comparing the EDT efficiency after weld cooling (at $T = 20$ °C, line 1) and in the process of welding ($T = 150$ and 300 °C, lines 2, 3).

According to the results of previous experimental studies, it was found that the electrode-indenter received a value $V_0 = 5$ m/s, and its temperature in the process of welding did not exceed 20 °C [7]. Therefore, the properties of the electrode-indenter at its contact interaction with the plate were set exclusively for $T = 20$ °C (Table 1, line 4).

Table 1. Mechanical characteristics of structural elements of EDT model of AMg61 alloy in the process of welding

Number	Structural element of the model	Material	Density ρ, kg/m³	Poisson's ratio, μ	*T*, °C	Modulus of elasticity *E*, GPa	Yield strength σ_y, MPa	Relative elongation δ,%
1	Plate of 300×200×3 mm	AMg61	640	0.34	20	71	150	22
2					150	60	120	40
3					300	55	50	55
4	Electrode of 15 mm diameter	M1	8940	0.35	20	128	300	6

The choice of T values is predetermined by the results of [12], where the mechanism of EDT action on the relaxation of stresses $\Delta\sigma$ of the plane specimens of AMg61 alloy during their load with longitudinal (along the main axis of the specimen) tension σ_0 was studied. The work shows that the maximum values $\Delta\sigma$ that determined the efficiency of treatment were achieved during tension of the specimens to $\sigma_0 = \sigma_y$.

Welding heating creates thermal expansion of metal in the treatment zone. According to the data of Table 1, at an increase in T, the values of elasticity σ_y of AMg61 alloy decrease, and plasticity δ increase. This, based on the results [12], contributes to intensification of the process of relaxation $\Delta\sigma$ of residual welding stresses at lower values σ_y at a constant energy level E_{EDT} of electrodynamic action. I.e., at E_{EDT} = const, the values $\Delta\sigma$ have an inverse dependence on σ_y. The relaxation mechanisms are based on the synergy of the electroplasticity effect and superposition of the wave of elastic stresses from EDT with the field of residual welding stresses [3, 12].

The justification of the choice of the range T was based on the following provisions. At $T = 150$ °C (Table 1, line 2), AMg61 alloy maintains elastic properties, that makes the contribution of the elastic wave of stresses to the relaxation of stress states dominant as compared to the electroplastic component. At $T = 300$ °C (Table 1, line 3), the opposite is observed, i.e. AMg61 alloy has high plasticity at low elasticity. This makes the plastic component in the process of stress relaxation dominant. Modeling of stress states at different T values allows optimizing the conditions of thermal effect on the action of EDT in the process of welding.

Welding stresses in the plane of the plate were modeled by setting the values of longitudinal σ_x (along the axis x in Figure 1) and transverse σ_y (along the normal to the axis x) components of tensile stresses. The values σ_x and σ_y were respectively accepted equal to σ_y and $0.5\sigma_y$ of AMg61 alloy at $T = 20, 150$ and 300 °C. The result of modeling is the distribution of components σ_x and σ_y of temporary and residual stresses over the thickness of the plate in the points B, C between them after its dynamic loading along the axis z, as is shown in Figure 3. The distribution of temporary and residual σ_x and σ_y was modeled at a distance of 5 mm from the line B–C on both surfaces of the plate and between them. This allowed determining the nature of EDT action distribution from the line B–C over the thickness of the plate.

The distribution of stresses σ_x and σ_y along the line B–C (Figure 3) and at a distance of 5 mm from it after EDT at $T = 20, 150$ and 300 °C were considered.
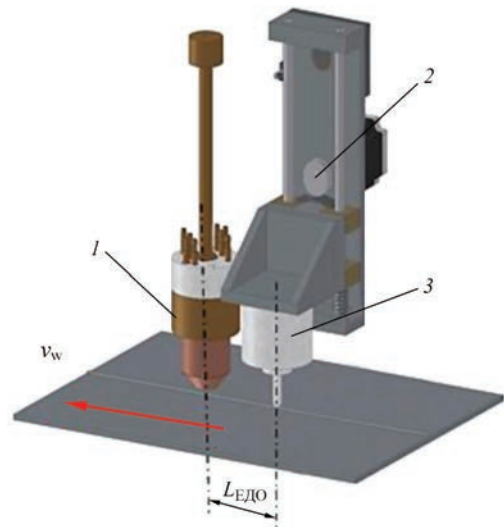

Figure 2. Scheme of EDT in the process of welding: v_w — welding direction; *1* — welding torch; *2* — eccentric; *3* — electrode device of EDT; L_{EDT} — distance between the axes of electrodes for welding and EDT

Figure 3 shows the results of modeling distribution of stresses σ_x and σ_y in the form of axonometric surfaces in the cross-section of the plates $\delta = 3$ mm at the moment of completion (instant patterns) of the EDT contact action at a temperature $T = 20, 150$ and 300 °C. Figure 3 shows the values of stresses along the line between the points B and C and at a distance of 5 mm from the line B–C. Analyzing the results of Figure 3 in general, it is possible to see the dominance of compression stresses throughout the whole considered temperature range both on the section B–C (i.e., along the contact action line) and at a distance of 5 mm from it.

The temperature effect on the plates of AMg61 alloy in the conditions of contact interaction with the indenter causes certain features of the formation of stress-strain states of the specimens to be considered below.

Figure 4 presents distribution of stresses σ_x along the line between the points B and C (Figure 1) of the plates of AMg61 alloy $\delta = 3$ mm after EDT at a variation of temperature effect T. The feasibility of studying the component σ_x is associated with its dominant effect on service characteristics of welded joints [2].

In Figure 4, *a, b* it can be seen that near the middle of the plane of the plate ($z = \delta/2$), an increase in the values σ_x in relation to stresses in the points B and C occurs. This is explained by the effect of reflection of stress wave at EDT from the absolute rigid base *3* (see Figure 2). The mathematical model of the reflection mechanism and verification of the results of the calculation at $T = 20$ ° C is considered in [11].

Using the data from Table 1, the analysis not of the absolute values of stresses σ_x and σ_y was carried out, but those derived with respect to σ_y. This, given the dependence $\sigma_y = f(T)$, allowed carrying out the correct
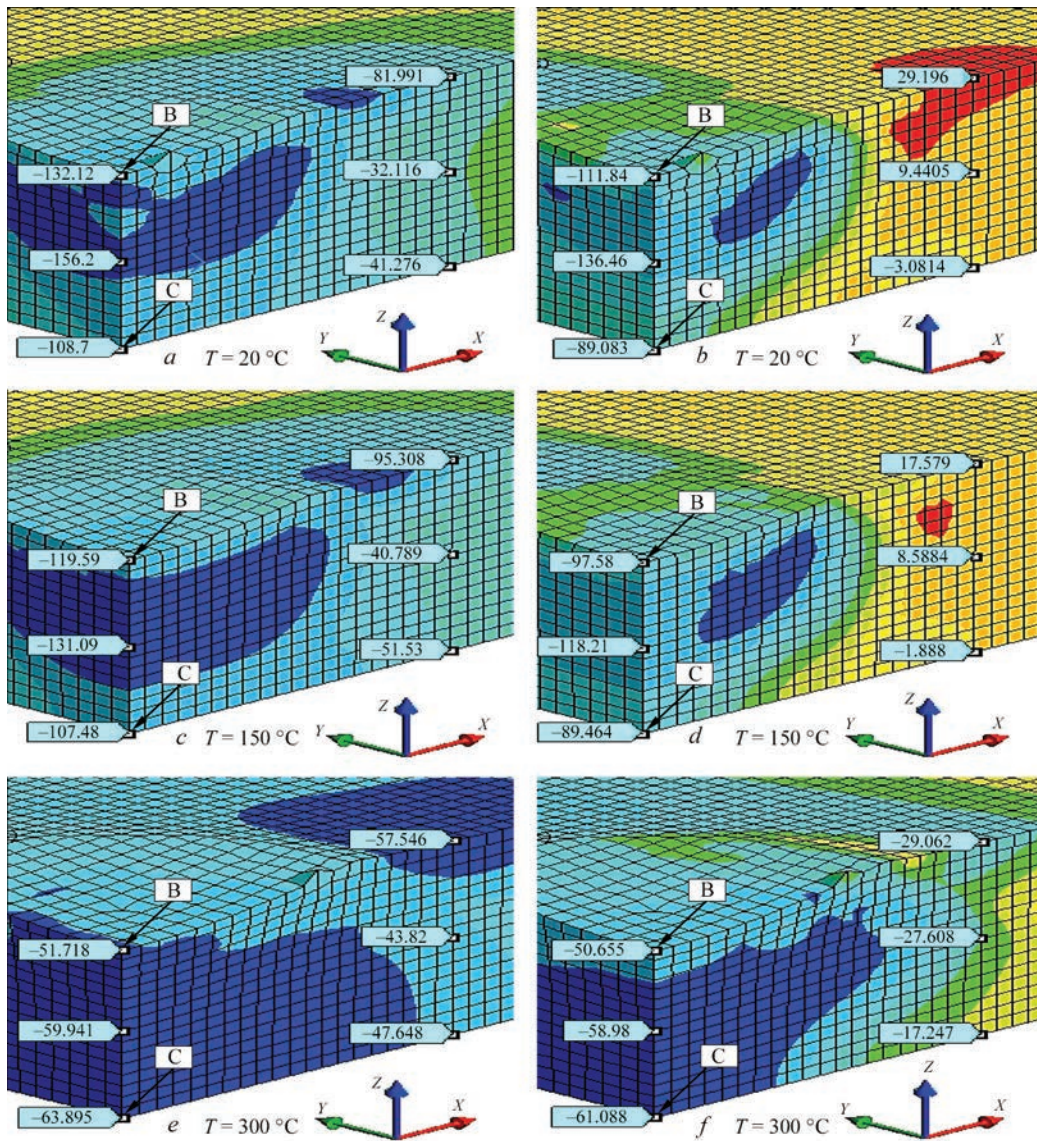
Figure 3. Instantaneous patterns of calculated distribution of values (MPa) of components of stresses σ_x, σ_y in the plate of AMg61 alloy $\delta = 3$ mm at the moment of completion of the EDT action along the line between the points B and C (Figure 2) and at a distance of 5 mm from the line B–C: a — σ_x at $T = 20$ °C; b — σ_y at $T = 20$ °C; c — σ_x at $T = 150$ °C; d — σ_y at $T = 150$ °C; e — σ_x at $T = 300$ °C; f — σ_y at 300 °C

comparative evaluation of the effect of variations of T values on EDT efficiency.

At 20 °C along the line B–C, the values σ_x and σ_y of compression stresses in the point B are higher than in the point C (Figure 3, a, b). Thus, in the point B, σ_x reaches the values $-0.88\sigma_y$ and in the point C $-0.75\sigma_y$ and σ_y in the point B reaches $-0.74\sigma_y$ and $-0.6\sigma_y$ in the point C. At the area of the cross-section, which corresponds to half of the thickness of the plate (further — area $\delta/2$), σ_x and σ_y reach the values, respectively $-\sigma_y$ (Figure 4, a for σ_x) and $-0.9\sigma_y$. I.e., the area near the middle of the plate ($z = \delta/2$) is subjected to the maximum effect of σ_x and σ_y stresses after EDT at $T = 20$ °C.

While removing from the line B–C by 5 mm, a decrease in stresses and a change in the nature of their distribution over the thickness of the plate is observed (Figure 3, a, b). Thus, the compression σ_x

reaches $-0.55\sigma_y$ in the point B and $-0,27\sigma_y$ — in the point C. In the area $\delta/2$, σ_x reach $-0.2\,\sigma_y$. At the same time, while removing by 5 mm from the line B–C, σ_y are tensile, which reach $0.2\sigma_y$ in the point B, monotonously reduced to $0.06\sigma_y$ in the point $\delta/2$ and almost to zero in the point C.

An increase in the treatment temperature to 150 °C (Figure 3, c, d) has a positive effect (as compared to $T = 20$ °C) on the value and the nature of distribution of compression stresses in the cross-section of the plate. At the same time, the area of action of compression stresses σ_x on the cross-section of the plate is slightly larger than the area of action at $T = 20$ °C (Figure 3, a, b). In the point B, compression σ_x and σ_y, as well as at $T = 20$ °C, are larger than on the reverse one. Thus, in the point B, the values σ_x and σ_y reach respectively $-\sigma_y$ and $-0.8\sigma_y$ of AMg61 alloy at

$T = 150\ °C$ and -0.95 and $-0.77\sigma_y$ during cooling to $T = 20\ °C$ (Figure 4, *b* for σ_x). In the point $\delta/2$, the values σ_x and σ_y reach σ_y for temperatures $T = 150$ and $20\ °C$. In the point B, σ_x reach $-0.85\sigma_y$, $\sigma_y = -0.71\sigma_y$ at $T = 150\ °C$ and $\sigma_x = -0.89\sigma_y$, and $\sigma_y = -0.74\sigma_y$ at $T = 20\ °C$ (Figure 4, *b* for σ_x).

While removing by 5 mm from the line B–C, as in the previous case, the compression stresses on the facial side of the plate are higher than the absolute value unlike on the side of the backing plate. At $T = 150\ °C$, the maximum compression values σ_x in the point B reach $-0.8\sigma_y$ (Figure 3, *c*) and during cooling to $20\ °C$, they reach $-0.75\sigma_y$. At $T = 150$ and $20\ °C$, the maximum values of tensile σ_y on the contact surface reach $0.15\sigma_y$. On the area $\delta/2$, the values of compression σ_x reach $-0.34\sigma_y$, and tensile σ_y, respectively, $0.07\sigma_y$ for temperatures 150 and $20\ °C$. In the point C, the compression σ_x reach $-0.43\sigma_y$ and σ_y are close to zero in the considered temperature range. The distribution of σ_y over the cross-section of the plate increases slightly, as compared to the results of Figure 3, *b*. While comparing the values σ_x while removing by 5 mm from the line B–C at $T = 20$ and $150\ °C$, it can be seen that the thermal effect contributes to the formation of greater compression stresses than after EDT at room temperature.

As compared to EDT at $T = 20\ °C$, it can be seen that an increase in the treatment temperature to $300\ °C$ (Figure 3, *e, f*) promotes the distribution of compression stresses over the thickness of the plate and reduction of their values as compared to the results at $T = 20$ and $150\ °C$ (Figure 3, *a–d*). In the point B, the values of σ_x and σ_y of compression stresses, unlike the previous variants, are lower than in the point C and reach $-\sigma_y$ at $T = 300\ °C$ and $-0.44\sigma_y$ during cooling to $T = 20\ °C$ (Figure 4, *c* for σ_x). In the point $\delta/2$, compression σ_x and σ_y reach the values $-\sigma_y$ for $T = 300\ °C$ and $-0.54\sigma_y$ for $T = 20\ °C$. In the point C, compression σ_x and σ_y reach $-\sigma_y$ at $T = 300\ °C$ and $-0.5\sigma_y$ at $T = 20\ °C$. At the same time, the area of action of
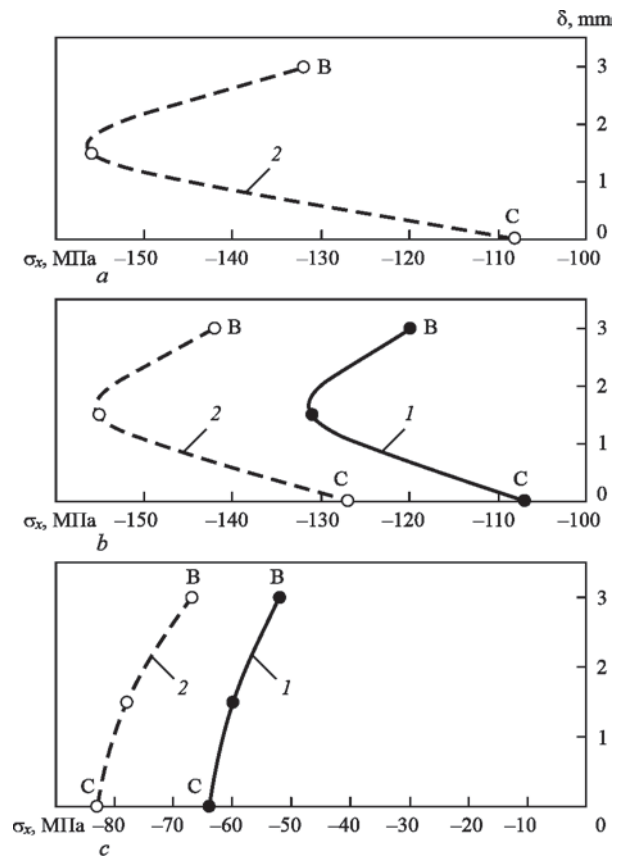

Figure 4. Stresses σ_x along the line between the points B and C (Figure 2) of plates of AMg61 alloy $\delta = 3$ mm after EDT at a temperature T and cooling to $T = 20\ °C$, where the curve *1* — σ_x (instantaneous) at the moment of completion of contact interaction at elevated temperatures; curve *2* — σ_x at room temperature: *a* — $T = 20\ °C$; *b* — 150; *c* — 300

stresses σ_x (Figure 3, *d*) over the cross-section of the plate three times increases as compared to the variant of EDT at $T = 20\ °C$ (Figure 3, *a*).

While removing by 5 mm from the line B–C, as in the previous variants of the calculation, the reduction of stresses (Figure 3, *e, f*) is determined. Thus, the maximum values of the compression σ_x in the point B reach $-\sigma_y$ at $T = 300\ °C$. During cooling to $T = 20\ °C$, the compression σ_x in the point B reach $-0.49\sigma_y$ (Figure 4, *c*). The stresses σ_y while removing by 5 mm

Table 2. Relative values of stress components σ_x and σ_y in the plate of AMg61 alloy $\delta = 3$ after EDT at the variation of values of temperature T of its accompanying heating

Number	T, °C	Line B–C						5 mm from the line B–C					
		σ_x			σ_y			σ_x			σ_y		
		B, $\times\sigma_y$	$\delta/2$, $\times\sigma_y$	C, $\times\sigma_y$	B, $\times\sigma_y$	$\delta/2$, $\times\sigma_y$	C, $\times\sigma_y$	5 mm from the B $\times\sigma_y$	5 mm from the $\delta/2$ $\times\sigma_y$	5 mm from the C $\times\sigma_y$	5 mm from the B $\times\sigma_y$	5 mm from the $\delta/2$ $\times\sigma_y$	5 mm from the C $\times\sigma_y$
1	20	−0.88	−1.0	−0.75	−0.74	−0.9	−0.6	−0.55	−0.2	−0.27	0.2	0.06	0
2	150	−1.0	−1.0	−0.85	−0.8	−1.0	−0.71	−0.8	−0.34	−0.43	0.15	0.07	0
3	20 after cooling from $T = 150\ °C$	−0.95	−1.0	−0.89	−0.77	−1.0	−0.74	−0.75	−0.34	−0.43	0.15	0.07	0
4	300	−1.0	−1.0	−1.0	−1.0	−1.0	−1.0	−1.0	−0.88	−1.0	−0.6	−0.54	−0.34
5	20 after cooling from $T = 300\ °C$	−0.44	−0.54	−0.5	−0.44	−0.54	−0.5	−0.49	−0.38	−0.41	−0.24	−0.24	−0.14

7

from the line B–C are compressive over the thickness of the plate in the range of T from 300 to 20 °C. On the surface near the point B at $T = 300$ °C, σ_y reach $-0.6\sigma_y$ and at $T = 20$ °C respectively $-0.24\sigma_y$.

In the point $\delta/2$, the compressions reach $-0.88\sigma_y$ at $T = 300$ °C and $-0.38\sigma_y$ at $T = 20$ °C (Figure 4, c). In the p $\delta/2$, the compressions σ_y reach the values $-0.54\sigma_y$ at $T = 300$ °C and $-0.24\sigma_y$ at $T = 20$ °C. On the surface near the point C, the compressions σ_x at $T = 300$ °C reach $-\sigma_y$, and at $T = 20$ °C they decrease to $-0.41\sigma_y$ (Figure 4, c). On the surface near the point C, compressions σ_y at $T = 300$ °C reach $-0.34\sigma_y$, and at $T = 20$ °C they also decrease to $-0.14\sigma_y$. Also, the distribution of σ_y across the cross-section of the plate increases significantly as compared to the results of Figure 3, b. When comparing the values of σ_y while removing by 5 mm from the line B–C at $T = 20$ and 300 °C, it should be noted that the thermal effect contributes to the expansion of the area of action of compressive stresses at a decrease in their values.

The results of modeling described above are summarized in Table 2. When comparing the lines 1 and 2 and 1 and 4, it can be seen that the thermal action, which accompanies EDT, initiates more instantaneous values of stresses (in relation to σ_y) at elevated temperatures as compared to σ_x and σ_y at $T = 20$ °C. This contributes to the formation of higher compressive stresses during cooling of the plate as compared to the stress state after EDT at $T = 20$ °C. When comparing the lines 1 and 3, it can be seen that EDT of the plates of AMg61 alloy $\delta = 3$ mm under the conditions of their thermoelastic heating (at $T = 150$ °C) is more effective than at $T = 20$ °C. However, at EDT at the temperature of thermoplasticity ($T = 300$ °C), high values of instantaneous stresses, which are comparable to σ_x and σ_y at $T = 150$ °C (respectively, lines 4 and 2), form significantly lower residual compressive stresses, which is seen at comparison of the lines 3 and 5. This fact can be explained by the fact that at low values σ_y at $T = 300$ °C (Table 1, line 3), relaxation processes take place less intensively than at elastic heating to $T = 150$ °C, which indicates the dominance of the elastic component in the formation of stress-strain states in EDT. This is confirmed by the results of [12], which proved that the most effective is EDT of plane specimens of AMg6 alloy, which were previously tensioned to σ_y. I.e., preheating of the specimens to $T = 150$ °C according to [12], contributes to the maximum efficiency of EDT.

CONCLUSIONS

1. It was proved that the use of electrodynamic treatment (EDT) of the weld metal, which is performed in a single process synchronously with fusion welding, is more effective as compared to separate EDT after welding, which is expressed in a more optimal residual stress-strain state of a finished welded joint.

2. On the basis of the previously developed mathematical model of the impact interaction of the electrode-indenter with the welded plate of AMg61 alloy, a numerical calculated evaluation of its stress states as a result of EDT at elevated temperatures was carried out.

3. Using the mathematical model of the mechanism of impact interaction of the electrode-indenter with the welded plate during EDT in the conditions of elevated temperatures in a plane two-dimensional statement, modeling of stresses at an impact elastic-plastic action of the electrode-indenter at a temperature of 20, 150 and 300 °C in the plate of AMg61 alloy with the thickness of 3 mm was performed. It was established that the most satisfactory stress state (among investigated) corresponds to EDT at a temperature of 150 °C.

REFERENCES

1. Madi, Y., Besson, J. (2014) *Effect of residual stresses on brittle fracture*. Mat. ECRS-9. UTT, Troyes, France.
2. Masubuchi, K. (1980) *Analysis of welded structures, Pergamon Press*, Oxford, United Kingdom.
3. Lobanov, L.M., Pashchyn, N.A., Kondratenko, I.P. et al. (2018) Development of post-weld electrodynamic treatment using electric current pulses for control of stress-strain states and improvement of life of welded structures. *Materials Performance and Characterization*, **7**, 4. DOI: https://doi.org/10.1520/MPC20170092. ISSN 2379-1365
4. Lobanov, L.M., Pashchyn, M.O., Tymoshenko, O.M. et al. (2020) Increase in the life of welded joints of AMg6 aluminium alloy. *The Paton Welding J.*, **4**, 2–8. DOI: https://doi.org/10.37434/as2020.04.01
5. *Conrad H.*, Sprecher A. (1989) *The electroplastic effect in metals.* Elsevier Science Publishers B.V., Dislocations in Solids Ed. by F.R.N. Nabarro, 500–529.
6. Stepanov, G.V., Babutskii, A.I., Mameev, I.A. (2004) High-density pulse current-induced unsteady stress-strain state in a long rod. *Strength of Materials*, **36**, 377–381. DOI: https://doi.org/10.1023/B:STOM.0000041538.10830.34
7. Lobanov, L.M., Pashchyn, M.O., Mykhodui, O.L., Sydorenko, Yu.M. (2017) Effect of the indenting electrode impact on the stress-strain state of an AMg6 alloy on electrodynamic treatment. *Strength of Materials*, 49(**3**), 369–380. DOI: https://doi. org/10.1007/s11223-017-9877-1
8. Sydorenko, Y.M., Pashchyn, M.O., Mykhodui, O.L. et al. (2020) Effect of pulse current on residual stresses in AMg6 aluminium alloy in electrodynamic treatment. *Strength of Materials*, 52(**5**), 731–737. DOI: https://doi.org/10.1007/s11223-020-00226-2
9. Lobanov, L.M., Pashchin, N.A., Mikhodui, O.L., Sidorenko, Y.M. (2018) Electric pulse component effect on the stress state of AMg6 aluminium alloy welded joints under electrodynamic treatment. *Strength of Materials*, 50(**2**), 246–253. DOI: https://doi.org/10.1007/s11223-017-9862-8 10
10. http://www.ansys.com/
11. Lobanov, L.M., Pashchyn, M.O., Mikhodui, O.L. et al. (2021) Modeling of stress-strain states of AMg6 alloy due to impact action of electrode-indenter in electrodynamic treatment. *The Paton Welding J.*, **6**, 2–11. DOI: https://doi.org/10.37434/tpwj2021.06.01

12. Lobanov, L.M., Pashchyn, M.O., Mikhodui, O.L. (2012) Influence of the loading conditions on the deformation resistance of AMg6 alloy during electrodynamic treatment. *Strength of Materials*, **44**, 472–479. DOI: https://doi.org/10.1007/s11223-012-9401-6

ORCID

L.M. Lobanov: 0000-0001-9296-2335
M.O. Pashchyn: 0000-0002-2201-5137,
O.L. Mikhodui: 0000-0001-6660-7540,
E.V. Illyashenko: 0000-0001-9876-0320,
P.V. Goncharov: 0000-0002-1980-2340

CONFLICT OF INTEREST

The Authors declare no conflict of interest

CORRESPONDING AUTHOR

M.O. Pashchyn

E.O. Paton Electric Welding Institute of the NASU
11 Kazymyr Malevych Str., 03150, Kyiv, Ukraine.
E-mail: svarka2000@ukr.net

DEVELOPED in PWI

EQUIPMENT FOR ROBOTIC SPOT PLASMA WELDING ON ASYMMETRIC ALTERNATING CURRENT AND DIRECT CURRENT STRAIGHT POLARITY

Spot welding is performed by a plasma arc on alternating asymmetric current to join materials with a refractory oxide film on the surface (aluminum, magnesium and beryllium alloys) or on direct current of direct polarity to join materials without a refractory oxide film on the surface (low alloy steels, stainless and high strength steels, titanium, copper alloys). Spot joints are formed both without and with the use of filler wire feed.

The use of this equipment allows:

► to produce lightweight hollow structures (density is lower by 30–60 % compared to solid alloys), which consist of several sheets of high-strength aluminum and magnesium alloys with alternating sheets and truss (embossed) intermediate layers;

► welding sheets in a multilayer honeycomb panel with a thickness of 0.5 to 3.0 mm, welding sheets to a thinner corrugated filler, obtaining a honeycomb multilayer panel up to 4 meters wide and up to 12 meters long;

► to produce lightweight curvilinear panels by bending the first sheet of the panel according to a template, to obtain the required surface shape while ensuring high structural rigidity.
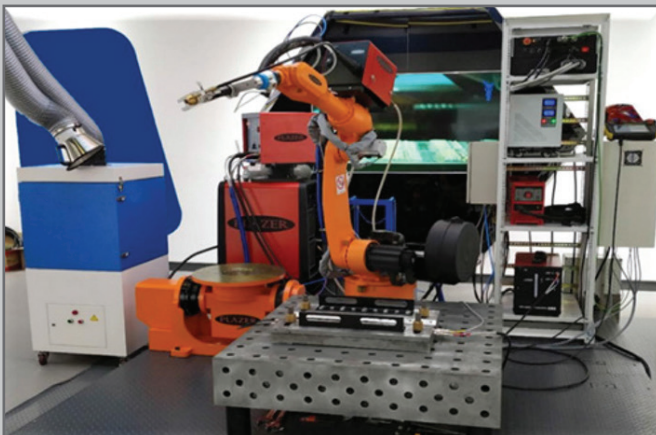
Robotic complex (left) and plasma torch (right) with a pneumatic clamping mechanism for spot plasma welding with direct and alternating asymmetric current of increased frequency